Sharp images of WR104

Soulain A.[a], Millour F.[a], Lopez B.[a], Lagadec E.[a], Matter A.[a], and Hofmann K.-H.[b]

[a]Laboratoire Lagrange, UMR 7293 UNS-CNRS-OCA, Boulevard de l'Observatoire, CS 34229, 06304 Nice Cedex 4, France
[b]Max Planck Institute for Radio Astronomy, auf dem Hügel, 69, 53121 Bonn, Germany

ABSTRACT

Some carbon-rich Wolf-Rayet stars are permanent dust producers, as seen by their infrared excess. In famous targets like WR104, the dust is found in the form of a pinwheel nebula around the central source, providing an indirect evidence of binarity. WR104 has been studied in details with the Keck, and more recently with the VLTI by our team. We present here images obtained with the SPHERE instrument and last modelling efforts based on AMBER data. First results shown that the pinwheel appears to be diluted by diffuse emission. Moreover, a minimum distance between the central binary and the dust-formation zone appears necessary to reproduce both AMBER and SPHERE data.

Keywords: Wolf-Rayet stars, pinwheel nebulae, model fitting, interferometry.

1. INTRODUCTION

1.1 Wolf-rayet stars

Wolf-Rayet stars (WR) are luminous massive blue stars with strong and optically thick stellar winds. This highly supersonic winds due to radiation pressure onto the gaz of the stellar atmosphere exerts a major influence on their immediate surroundings. As a consequence, these stars show many emission lines of nitrogen and helium for WN stars, and of carbon, oxygen and helium for WC stars. WC8 and WC9 exhibit a strong infrared excess, evidence of hot and warm dust emission (Allen et al. 1972[1]), produced by the central source. These WR dust makers have a very high dust-formation rate contributing to the enrichment of interstellar medium. This rate can reach values up to $\dot{M} = 10^{-4} M_{\odot}/yr$ (Puls et al. 2008[2]). The wind-wind collision zone between the WR and the O component present in these systems offers ideal condition to reach critical densities to enable the formation of dust, explaining the large infrared emission from binaries and the spiral structures observed around some "pinwheel nebulae" (WR104, WR98a or WR118). This newly produced dust created around the shock follows then a ballistic trajectory forming an Archimedian spiral pattern described in details by Tuthill et al. (2008[3]).

1.2 Pinwheel nebulae : the peculiar WR104

We present some work in progress on the prototype star WR104, which is the most studied dusty WR star so far. It was discovered as a "pinwheel" dusty nebula by Tuthill (1999[4]). It was observed in a follow-up series of observations,[3] confirming its binarity and refining most of its parameters. Major results are the orbital period 241.5 ± 0.5 days, the angular outflow velocity of 0.28 ± 0.02 mas/day and an optically thin cavity of angular size 13.3 ± 1.4 mas corresponding to the distance between the central binary star and the dust creation-zone. Such atypical dust shells are a remarkable problem for the theory of dust production, several hydrodynamical and radiative transfer models were made to explain the pinwheel pattern around WR104 (Harries et al. 2004[5] ; Lamberts et al. 2012[6]). Many aspects of this curious object are still to be understood and new instruments allow us to progress. Specially, interferometric observations could reveal the dust-forming region and the geometrical width and thickness of the pinwheel arms. Associated with new modelling efforts, the physics of the object can be finally examined in more details.

2. NEW IMAGES OF WR104

2.1 SPHERE/near-infrared

2.1.1 Observations and data reduction

We observed WR104 with SPHERE/VLT. SPHERE is a high-performance Adaptive Optics system (AO) installed at the Nasmyth focus of Unit Telescope 3 of the Very Large Telescope. Our observations were obtained on the night of the 3^{rd} May in several filters across the H band with IRDIS, and at YJ (0.95-1.35 μm, spectral resolution R $\approxeq$ 54) with the Integral Field Spectrometer. We observed WR104 and a point spread function (PSF) calibrator, 4Sgr (HD163955, spectral type B9V). 4Sgr is unresolved by IRDIS ($\lambda/D \approx$ 30-35 mas, while $\theta_{UD} = 0.40 \pm 0.03$ mas) based on surface brightness relation (*Searchcal/JMMC*; Bonneau et al. 2006[7]). The observation required 2h of telescope time and were taken without coronograph. Due to the extreme brightness of WR104 in H-band, a neutral density ND2 was necessary in all filters. All images were taken using dithering technique, consisting in shifting the target on detector between different integrations (a 4×4 pattern was used with a shift of 1 or 2 pixels). A total of 97 cubes were recorded on WR104 (with 2×5 images in classical imaging mode with the same filters in both part of detector) and 32 cubes (in DBI mode) with a plate scale of 12.27 mas/pixel.

We performed the data reduction using our own pipeline reduction software made in python. It consists of standard calibrations and cosmetics process (dark current, flat field, bad pixel map, etc.). All frames are then shifted, added and averaged using dithering informations and Fourier cross-correlation. The resulting image is shown in Fig.1.

2.1.2 Reduced images

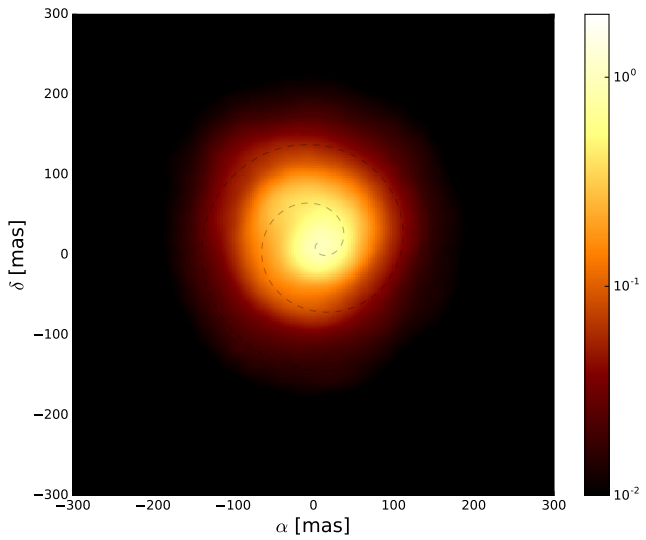


Figure 1. Reduced normalized image of WR104 in H band (1.66μm). The spiral signature is clearly identified. These observations are the first direct classical imaging of the spiral around WR104.

The reduced SPHERE images exhibit the spiral structure around the central system well represented by an archimedian spiral seen approximately face-on (see dashed line in Fig.1). An over-resolved component can be seen in all filters with an apparent size increasing at larger wavelength. The orientation and global size of the object are consistent with previous observations (Tuthill, Monnier et al. 2004[3]). We find exactly the expected orientation using the previous results and a periodical rotation rate of 241 days since the previous observations in June 1998.

2.1.3 Geometrical model

In order to interpret the interferometric data obtained with the VLTI/AMBER and MIDI interferometers, we developed a toy model aiming at generating visibilities and images for a variety of parameters : disk, ring, unresolved star, binary, pinwheel, etc. Preliminary studies of VLTI/AMBER data of WR104 by our team revealed that the pinwheel seems diluted by diffuse emission in the system, and we found that there is likely a point source in the middle of the system in the H-band data, at a level larger than 5% of the total flux. With these information, we made a model formed by a pinwheel, an unresolved source (central binary WR+O) and a Gaussian envelope (diffuse emission).

The pinwheel is formed by a succession of rings growing linearly and following an Archimedian spiral pattern (Millour et al. 2008;[8] Millour et al. 2009[9]). We add from these previous works, a different ring contribution determined using blackbodies at distinct temperatures following a power law. All rings flux are then normalized by the total flux. In line with Tuthill's observations, we decided to add also a distance between the central binary star and the first ring, named Shock distance (d_{shock}).

The flux contributions of the three components are calculated at different wavelength using blackbodies. We chose 70000K for the WR star, 30000K for the O star and 1200K for the pinwheel (Harries et al. 2004[5]). The envelope component is taken to be independent of wavelength. All relative fluxes are then calculated using scale parameters and the total flux. All parameters of our model are presented in Tab.1 (for more details, see also Fig.5).

Parameters	Description	Previous works	This work
Rounds	Number of spiral turns	1	1
Opening angle	Opening angle of the front shock imposed by the last ring thickness	41	42
totalSize	Distance between O+WR and last ring	≈60 mas	65 mas
power	Power of the spiral, 1 for an Archimedian	1	1
angleSky	Orientation in the sky	-	-
incl	Inclinaison from face-on viewing angle	≤16°	11°
d_{shock}	Distance between star and first ring	13.3 ± 1.4 mas	12.5 mas
d_{bin}	Binary separation	≈1 mas	≈1 mas
T_{sub}	Sublimation temperature of dust	1200 K	1200 K
q	Power of temperature law	0.4	0.35
a_{star}	Scale parameters of relative star flux	-	-
a_{pwhl}	Scale parameters of relative pinwheel flux	-	-
a_{env}	Scale parameters of relative envelope flux	-	-
FWHM	Envelope size	-	100 mas

Table 1. Parameters of the model used to describe WR104. The new aspect of the model are represented in blue. We dispose of a large number of parameters and all the difficulties come from the low quantities of data.

2.1.4 Model comparison

We used the SPHERE data of WR104 and its associed PSF to make a comparison between our model and the data. The SPHERE data are very important to constrain large scale structures and the orientation of WR104.

The data can be reproduced using our model and a relative contribution of 5% for the star, 45% for the envelope and 55% for the pinwheel, with a sublimation temperature of 1200K and $q = 0.3$. Moreover, a distance

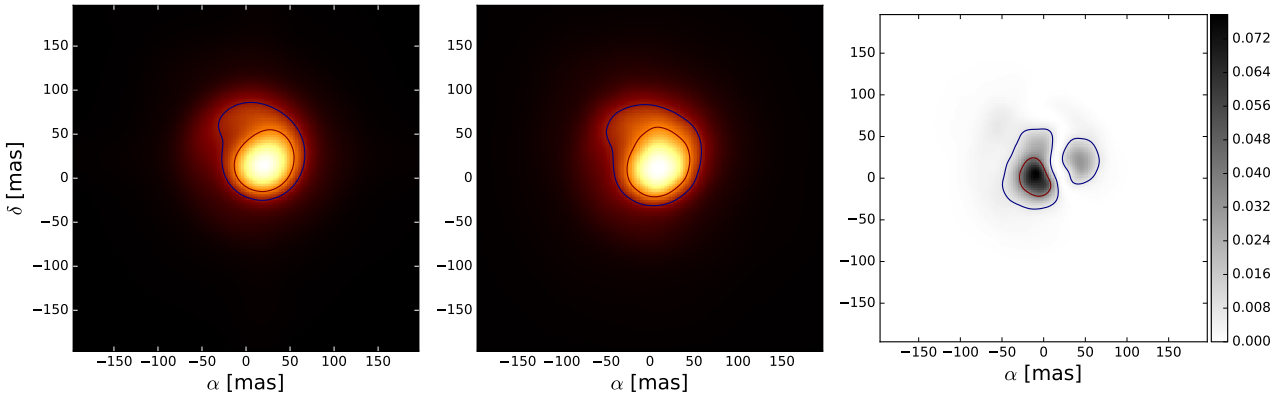


Figure 2. Comparison between geometrical model and data. **Left:** Model convolved by the PSF; **Middle:** Data in H band filters ($1.66\mu m$); **Right:** Squared residual corresponding to the substraction between data and model. Contour levels are 30 and 50% of the peak.

between the central star and the first ring of **≈12 mas** is necessary to reproduce the image. This minimum distance is also necessary for the AMBER data which reinforces the idea introduced by Tuthill (2004). It is important to note that the low spatial frequencies probed by SPHERE can not determine these parameters with high accuracy, the extended part of the envelope used here represented by the model gaussian component can be also attributed to the pinwheel at larger distance (second loop for instance).

2.1.5 Pushing the SPHERE image analysis through deconvolution

SPHERE is an instrument designed to directly detect planets around other stars than our very own Sun. This goal is reachable thanks to the extreme adaptive optics. The deconvolution approach is one of the specification to detect exoplanet and SPHERE is a perfect instrument to make images limited by the diffraction. We performed Lucy-Richardson and Wiener deconvolution to reach this limit.

We deconvolved the H band images of WR104 using the PSF associed with the Lucy-Richardson (L-R) algorithm implemented in python (Lucy 1974[10]). We stopped the deconvolution at 60 iterations, as the deconvolved images do not show significant evolution and due to increases of noises after 80 iterations. We also performed a Wiener deconvolution (Orieux et al. 2010[11]) to compare the results with the (L-R) algorithm (see Fig.3).*

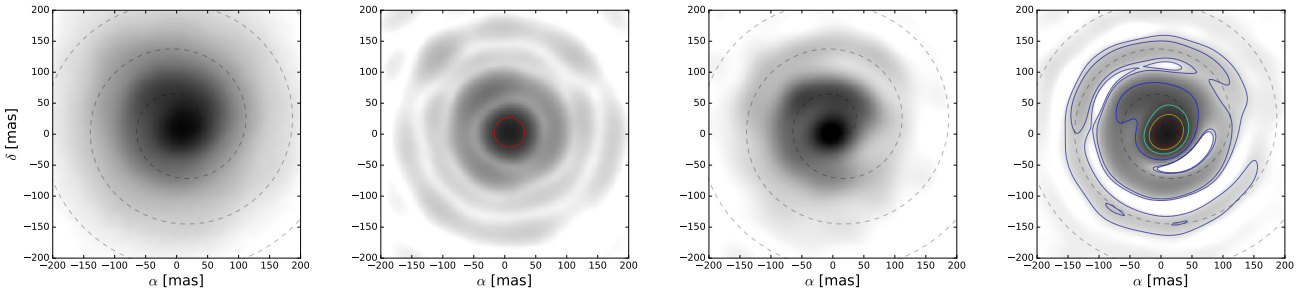


Figure 3. Example of deconvolution at 1.66 μm; All images are in log scale. **Left:** Reduced data; **Middle/left:** Reduced PSF with FWHM of 50 mas/Rayleigh criterium (red circle); **Middle/right:** Lucy-Richardson deconvolution (60 iterations); **Right:** Wiener deconvolution, contour levels are .5, 1, 10, 30, 50, 70% of the peak. We also represent the best archimedian spiral fit.

We can see that the two deconvolution technique show the same kind of structure assigned at the first and second loop of the pinwheel with a flux of 0.5-1% relative to the maximum. We can give an upper limit of the arms thickness around 30 mas.

*Skimage package; documentation: http://scikit-image.org

3. HIGH SPATIAL RESOLUTION

The direct imaging techniques used to described the complex system WR104 (SPHERE, VISIR) are really important to have an idea of the system as a whole, but the smallest details are invisible with the resolution of one single VLT telescope (42mas for H band). Only interferometry can probe inner regions of the system. During the last decade, several hydrodynamical and radiative transfer simulations were performed on WR104 and they need observational constrains. We have AMBER/VLTI data obtained on P88 and MIDI/VLTI obtained on P77. Although these data appear to be extremely difficult to interpret because of the sparse UV coverage and the aligned configuration used with the ATs, this first dataset allowed us to refine our model with more parameters.

3.1 VLTI/AMBER long-baseline interferometry

We used AMBER/VLTI, the near-infrared focal instrument of the VLTI, operates in the H and K bands (1.5 to 2.5 μm). AMBER can take profit of the spectral information to probe an important part of the UV plan. We obtained two epochs of observations with a linear baseline configuration, with projected baselines ranging from 10 to 40 m. Fig.4 presents the AMBER squared visibilities between 1.5 and 2.5μm with their corresponding model.

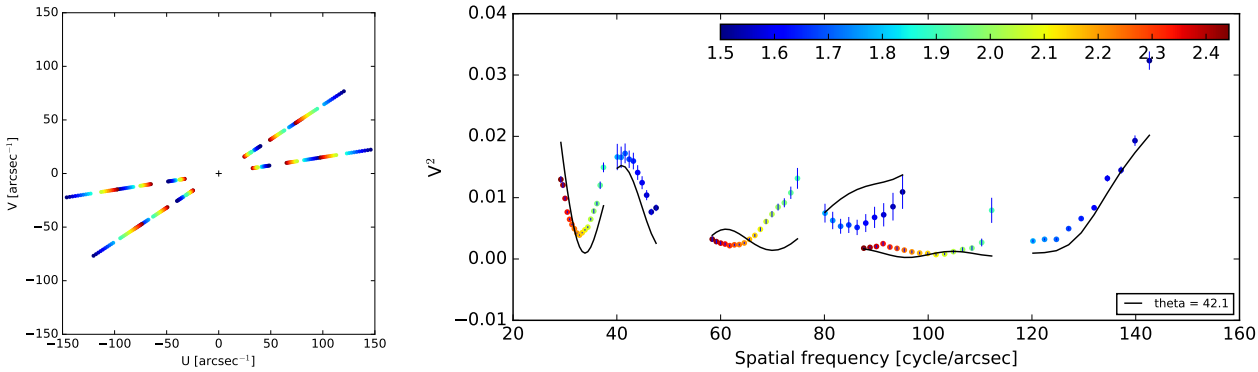


Figure 4. Visualisation of AMBER data. **Left:** UV plan; **Right:** Squared visibility and model fitting (work in progress).

These data show some interesting results which are consistent with the SPHERE data:

- Visibilities show an **unresolved component** contributing between 13% in the H band and 1% in the K band of the total flux. Highest spatial frequencies show this effect in the H band. This is in line with a star having 5% of the total flux seen in SPHERE.
- Totally resolved environment contributing at 10-15% of the total flux.
- Low visibilities at small spatial frequencies impose a distance shock at **11-13 mas**.
- Aperture angle $\theta \approx 42°$ with a last ring of 50 mas at a distance of 65 mas.
- Data show a good agreement with previous Harries[5] radiative transfer with a temperature of sublimation of **1200K** and a law temperature slightly lower $\mathbf{q = 0.35}$.

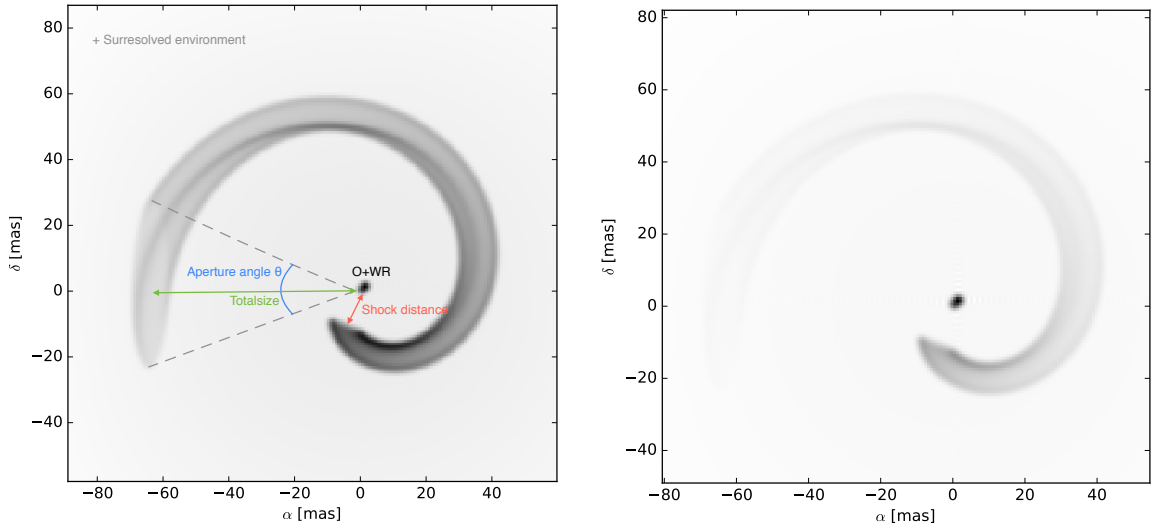


Figure 5. Model used to fit AMBER data (**left:** 2.4 μm; **right:** 1.6 μm). Important parameters are represented : aperture angle, totalsize and dust creation zone (shock distance). Contribution of the pinwheel is more important at longer wavelengths.

4. CONCLUSION AND PROSPECTIVES

New generation of instruments of the last decade enabled to study the curious object WR104 with many more details. Direct imaging with SPHERE can probe the large structure around the pinwheel and constrains some new aspects of the system like size, orientation, different flux contribution, etc.

High angular resolution can examine with more details the heart of the system with the detection of the dust formation zone. Coupled with hydrodynamical/radiative transfer modeling, we could determine the conditions of temperature, density and local radiation to define if dust creation is possible in such conditions.

As a near term perspectives, PIONIER/VLTI observations are plained in H band with all configuration (projected baselines ranging from 11 to 132m). These observation are planed between June and July 2016 and should probe in details the dust formation zone. We realized simulations of image reconstruction with the expected UV plan coverage and we obtained satisfying reconstructed images (Fig.6).



Figure 6. Expected PIONIER data and image reconstruction simulation with IRBIS software (Hofmann et al. 2014). **Left:** UV plan corresponding to our 25h obtained in ESO/P97; **Middle:** Our model at 1.66μm; **Right:** Reconstructed image.

Our team is implicated on the future MATISSE interferometer, currently developed at the *Observatoire de*

la Côte d'Azur in Nice, France. This new instrument will be able to observe in L, M and N bands. We will produce images in thermal infrared with highest resolution ever. Resolving dusty Wolf-Rayet stars is one of the science goals of the MATISSE instrument. As part of future scientific projects with MATISSE, we examined the expected number of WR star observable within the limit magnitude of the instrument. The future possibilities offered by this instrument will improve our knowledge on dusty WR, making possible survey studies on them (Fig.7).

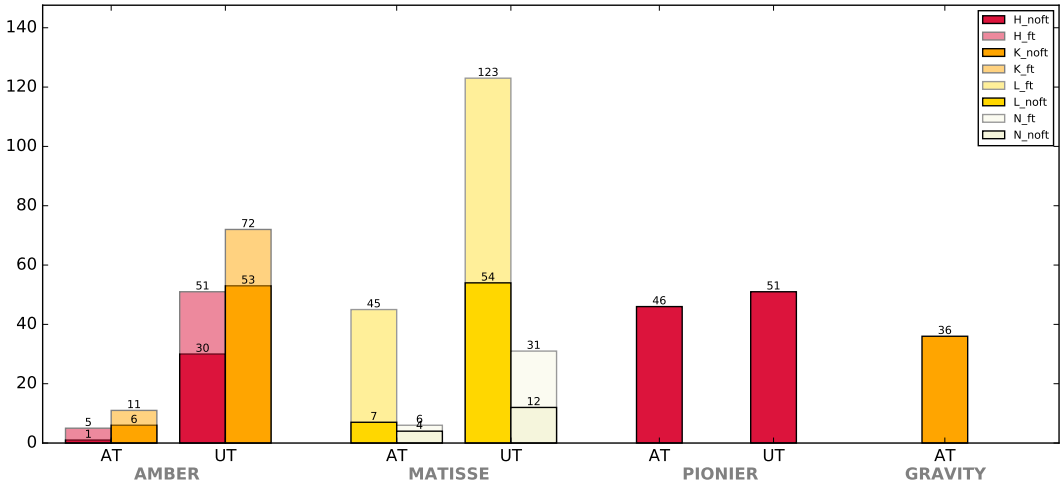


Figure 7. Future possibilities of MATISSE/VLTI to the studies of Wolf-Rayet star. MATISSE contribution is represented in yellow/write. The different numbers of observable WR stars are given with and without fringe tracking.

REFERENCES

[1] Allen, D. A., Swings, J. P., and Harvey, P. M., "Infrared photometry of northern wolf-rayet stars.," *Astronomy and Astrophysics* **20**, 333–336 (1972).

[2] Puls, J., Vink, J. S., and Najarro, F., "Mass loss from hot massive stars," *The Astronomy and Astrophysics Review* **16**, 209–325 (Dec. 2008).

[3] Tuthill, P. G., Monnier, J. D., Lawrance, N., Danchi, W. C., Owocki, S. P., and Gayley, K. G., "The Prototype Colliding-Wind Pinwheel WR 104," *The Astrophysical Journal* **675**, 698–710 (Mar. 2008).

[4] Tuthill, P. G., Monnier, J. D., and Danchi, W. C., "A dusty pinwheel nebula around the massive star WR104," *Nature* **398**, 487–489 (Apr. 1999).

[5] Harries, T. J., Monnier, J. D., Symington, N. H., and Kurosawa, R., "Three-dimensional dust radiative-transfer models: the Pinwheel Nebula of WR 104," *MNRAS* **350**, 565–574 (May 2004).

[6] Lamberts, A., Dubus, G., Lesur, G., and Fromang, S., "Impact of orbital motion on the structure and stability of adiabatic shocks in colliding wind binaries," *A&A* **546**, A60 (Oct. 2012).

[7] Bonneau, D., Clausse, J.-M., Delfosse, X., Mourard, D., Cetre, S., Chelli, A., Cruzalèbes, P., Duvert, G., and Zins, G., "SearchCal: a virtual observatory tool for searching calibrators in optical long baseline interferometry. I. The bright object case," *A&A* **456**, 789–789 (Sept. 2006).

[8] Millour, F., Valat, B., Petrov, R. G., and Vannier, M., ""Advanced" data reduction for the AMBER instrument," in [*Optical and Infrared Interferometry*], *Proceedings SPIE* **7013**, 701349 (July 2008).

[9] Millour, F., Driebe, T., Chesneau, O., Groh, J. H., Hofmann, K.-H., Murakawa, K., Ohnaka, K., Schertl, D., and Weigelt, G., "VLTI/AMBER unveils a possible dusty pinwheel nebula in WR118," *A&A* **506**, L49–L52 (Nov. 2009).

[10] Lucy, L. B., "An iterative technique for the rectification of observed distributions," *Astrophysical Journal* **79**, 745 (June 1974).

[11] Orieux, F., Giovannelli, J.-F., and Rodet, T., "Bayesian estimation of regularization and point spread function parameters for Wiener-Hunt deconvolution," *Journal of the Optical Society of America A* **27**, 1593 (June 2010).